Coordination Networks

DOI: 10.1002/anie.200802543

A Surface Coordination Network Based on Substrate-Derived Metal Adatoms with Local Charge Excess**

Greg Pawin, Kin L. Wong, Daeho Kim, Dezheng Sun, Ludwig Bartels,* Sampyo Hong, Talat S. Rahman, Robert Carp, and Michael Marsella

In the quest for increased control and tuneability of organic patterns at metal surfaces, more and more systems emerge that rely upon coordination of metal adatoms by organic ligands using endgroups such as carbonitriles, amines, and carboxylic acids.[1] Such systems promise great flexibility in the size and geometry of the surface pattern through choice of the ligand shape, the number and arrangement of ligating endgroups, and the nature of the metal centers. Planar (trigonal or square) arrangements of ligands around metal centers occur most commonly as a result of attractive interactions of the ligands with the substrate. In contrast, in the solution phase planar, and in particular trigonal planar, arrangements are quite rare and generally require ligands whose nature (for example bidentate, pincer shape) forces planarity.

Given the relatively short history of the field of surface coordination chemistry, compared to its solution-phase counterpart, it is of great interest to know which information can be gleaned from the latter to predict that for the former. Aspects of coordination chemistry at surfaces that have attracted very little attention to date are the effective oxidation state of the metal atom, which is much more straightforward to define in the solution phase, and the response of the coordination center to the presence of ligands at a surface.[2] This study details an effort at gaining some insight into these two aspects, using a coordination system which is particularly facile to prepare, as it relies on substrate atoms as coordination centers, rather than requiring their separate deposition.

In particular, this study describes the formation of a hexagonal network of 9,10-anthracenedicarbonitrile (DCA) on Cu(111) by titration of a nearly square molecular arrangement with copper atoms released from the substrate by annealing. We apply a combination of experimental and theoretical methods and juxtapose their results with the molecular patterns formed in the absence of a substrate.

Individual DCA molecules adsorb flat onto Cu(111) with the anthracene moiety parallel to the high-symmetry direction of the substrate. Figure 1 shows an STM image of DCA on Cu(111) and a simulation of the adsorption site (adsite) using density functional theory (DFT) on a 5 × 5 × 3 unit cell of substrate atoms. While the adsite of DCA resembles that of its oxygen[3] and sulfur[4] counterparts (anthraquinone and 9,10-dithioanthracene, respectively), DCA does not diffuse in a uniaxial fashion on Cu(111) and it also does not show more facile lateral manipulation along any particular substrate direction. Even at 90 K DCA retains sufficient surface mobility to assemble in patterns or to reach step edges.

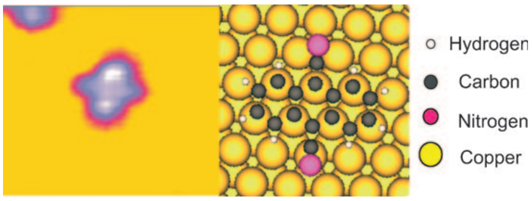

Figure 1. Left: STM image obtained at 25 K (35 × 30 Å, −1.9 V, 0.046 nA). Right: calculated adsorption geometry of DCA.

Increase of the DCA coverage leads initially to the formation of molecular rows followed by the formation of an ordered array of molecules featuring a nearly square unit cell, that is described in matrix notation as $\begin{pmatrix} 36 & 3 \\ -16 & 4 \end{pmatrix}$ (see Figure 2a, left, and Figure 2b). Each unit vector of this adsorbate pattern is 9.2 Å long and the angle between them is 88°, with a total of 15 substrate atoms per adsorbate. In this arrangement, all DCA molecules lie with the anthracene moieties in parallel, and adjacent rows of molecules in antiphase, bringing the nitrogen atoms of one row of molecules close to the terminal hydrogen atoms of two neighboring molecules (Figure 2d). For the purpose of this manuscript, we will refer to this pattern as the α phase.

Recently, we showed that hydrogen bonds of oxygen or sulfur atoms with terminal hydrogen atoms of anthracene

---

[*] G. Pawin, K. L. Wong, D. Kim, D. Sun, L. Bartels
University of California-Riverside
Pierce Hall, Riverside, CA 92521 (USA)
E-mail: ludwig.bartels@ucr.edu

K. L. Wong
University of California-Los Angeles
6266-D Boelter Hall, Los Angeles, CA 90095 (USA)

G. Pawin, D. Kim, L. Bartels, R. Carp, M. Marsella
Department of Chemistry
University of California-Riverside
Riverside, CA 92521 (USA)

S. Hong, T. S. Rahman
Department of Physics, University of Central Florida
Orlando, FL 32816 (USA)

[**] This work was supported by the US Department of Energy under grants DE-FGO2-03ER15464 (Bartels)/DE-FG02-07ER15842 (Rahman) and the US National Science Foundation 0647152 (Bartels/Marsella). Computational resources were made available by the San Diego Supercomputer Center.

Supporting information for this article is available on the WWW under http://dx.doi.org/10.1002/anie.200802543.

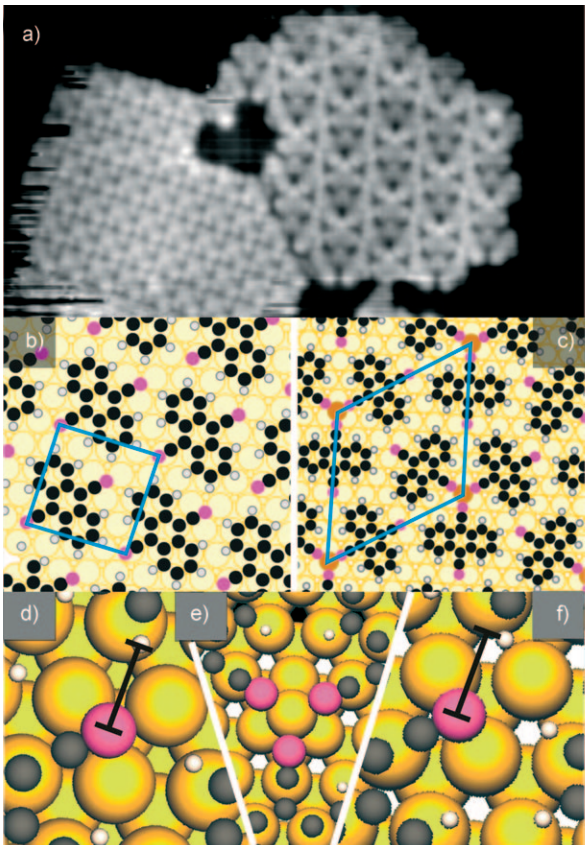

Figure 2. a) STM image of DCA on Cu(111) obtained at 180 K (175×95 Å, −2.6 V, 0.22 nA), depicting separate regions of the α phase (left) and β phase (right). b),c) DFT minimization of the adsorbate patterns (α and β phase) with the unit cell indicated. Because the unit cell in (c) is more than three times larger, only two substrate layers were included. d) Hydrogen bonding in the α phase. e) Coordination of a Cu adatom in the β phase. f) Increased N···H−C length in the β phase indicating the absence of hydrogen bonding. The calculations for the α and β phases used two and three substrate layers, respectively, leading to the difference in apparent background of panels (d), (e), and (f). Key as for Figure 1.

derivates on Cu(111) are associated with bond energies of 20-50 meV[5] and hydrogen-bond lengths of C−H···O of 2.8 Å.[6] In the case of DCA, the C−H···N length is somewhat longer, at 3.1 Å, yet each N atom is involved in two hydrogen-bonding interactions (in contrast to one bond for the referenced cases). To verify the presence of an attractive interaction between the nitrogen and the adjacent hydrogen atoms, we performed DFT calculations in which we placed two molecules on a 5×9×3 unit cell of substrate atoms, so that they either form two adjacent rows of molecules separated by empty space from the next double row, or so that they formed separated rows, thus allowing for hydrogen bonding in the first but not in the second case.[7] The first case has a lower total energy by 26 meV, indicating a hydrogen bond-energy of 0.01 eV, which is very small but reasonable for the system investigated.[5] We also find that, in the case of adjacent rows, the $C\equiv N$ bonds are elongated by approximately 5 pm towards their hydrogen-bond partners, as compared to separate rows, in further support of a local attractive interaction.

While previously reported metal-coordination networks at surfaces generally require a separate deposition step for the coordinating atoms, DCA/Cu(111) is more facile in its preparation. The continuous increase of the sample temperature at a rate of approximately 5 K per hour starting from 90 K leads to the formation of a new pattern at approximately 180 K. At this temperature a small amount of substrate atoms are thermally released from the substrate and form a two-dimensional layer of copper adatom gas that can interact with the DCA molecules[8] and form a coordination pattern. The amount of copper adatoms available for coordination then depends experimentally only on the temperature (and duration) of annealing. Figure 2a shows a sample at 180 K which, besides the aforementioned α phase, also features a DCA/Cu pattern on the right (β phase). This pattern incorporates one copper adatom for every three DCA molecules so that each DCA molecule is coordinated with copper only on one side and each copper atom is coordinated by three DCA molecules in a trigonal-planar arrangement. The resultant unit cell is $(\sqrt{48}\times\sqrt{48})\mathrm{R}30^\circ$ with 48 substrate atoms, three molecules, and one adatom per unit cell. It is noteworthy that the annealing procedure leads to an adsorbate pattern on the surface that is less dense than the original pattern (one DCA per 16 substrate atoms, as opposed to one DCA per 15 substrate atoms for the α phase).

We calculated the total energy of a 6×8×2 substrate-atoms supercell for the following cases: without any adsorbate, with a single Cu adatom, with the three DCA molecules in a trimer arrangement, and with the DCA molecules and a coordinated Cu adatom. Comparison shows that coordination provides a net binding energy of almost 1 eV (or 330 meV per Cu−N bond), substantially greater than the energy of the hydrogen bonds lost. A close inspection of the adposition of the coordinated molecules shows that the N···H−C bond length increased as a result of metal coordination of the opposite nitrogen atom (compare Figure 2d and Figure 2f). The inability of metal-coordinated DCA molecules to participate in a hydrogen-bonded network explains the separation of the adsorbate population into islands of pure and of metal-coordinated DCA molecules, despite the fact that these islands have a commensurate edge (see Figure 2a). Figure 2a also shows that the molecules are locked in place much more securely in the β phase, while the fuzzy edge of the α phase attests to constant attaching and detaching of molecules thereby contributing to a lattice gas of admolecules and adatoms that lets the β phase grow.

Titration of all DCA-nitrile groups with Cu atoms by means of annealing to room temperature for 100 min leads to formation of the γ phase (Figure 3), which can also be prepared directly by deposition of DCA at elevated temperatures. The 7×7 unit cell encompasses 49 substrate atoms, three DCA molecules, and two adatoms, one of which occupies an hcp site and the other an fcc site. The adsorption geometry of DCA closely resembles that of the previous two patterns. Notably, the DCA density on the substrate is further reduced, causing the STM image to reveal a pattern that resembles a honeycomb with apparently empty space surrounded by the DCA molecules.

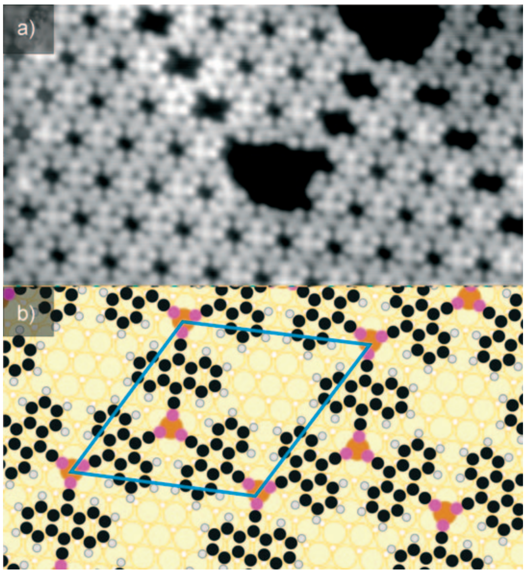

Figure 3. a) STM image (180×100 Å, −3.8 V, 57 pA, 30 K) of the γ phase of DCA on Cu(111). b) Corresponding model. Key as for Figure 1.

While the evolution from a hydrogen-bonded to an atom-coordination based network is readily explained by the associated binding energies, the reason for the transition from a nearly square to a trigonal network is not immediately apparent. While the sixfold symmetry of the substrate may favor a trigonal setup, there is no reason why the coordination-based pattern should reflect the substrate symmetry any more (or less) than the hydrogen-bonded one.

In contrast to surfaces, there is abundant data available on the coordination chemistry of metal atoms (including copper atoms and cations) in the solution phase, yet no copper DCA complexes have been reported to our knowledge. A statistical analysis of crystal structures[9] shows that copper complexes have an oxidation-state distribution of 38% Cu^I and 62% Cu^{II}. Of all complexes, only 13.8% are trigonal planar; 93% of these being the more reduced Cu^I. Except for cyanocuprate(I) networks,[10] trigonal-planar configurations occur only in the presence of bidentate ligands. Although DCA is not a bidentate ligand in this sense, it may still be illustrative to explore whether the coordination geometry of Cu adatoms at surfaces should resemble that of a monovalent cation in the solution phase, or whether closer resemblance to other oxidation states is found.

Relaxation of an uncoordinated Cu adatom on top of the 6×8×2 substrate unit cell in the context of the previously mentioned calculations produces a relaxation into the bulk of 0.2 Å, which is similar to that found in other calculations.[11] Unsurprisingly, integration of the charge density around the copper adatom over the Wigner–Seitz cell[12] surrounding it results in the same amount of charge found surrounding other surface atoms. However, in the case of a Cu adatom coordinated by three DCA molecules, no inward relaxation is found and integration of the charge density leads to an excess of one electron, even after subtracting the charge density of the neighboring nitrogen atoms.[13] While the extra charge density at the copper adatom explains the lack of inward relaxation, it is initially counterintuitive to the behavior generally expected of adatoms. It should by no means be interpreted as the copper atom withdrawing charge from DCA molecules; rather the Cu adatom appears to serve as a conduit allowing the DCA nitrogen atoms to interact effectively with the substrate electron density. In the course of this interaction, the adatom donates charge to the coordination bonds with the three nitrogen atoms. Given the size of the Wigner Seitz cell, which is based on the Cu–Cu distance (of 2.55 Å in the bulk), in comparison to the shorter Cu–N spacing (of 1.65 Å in the surface plane, 1.99 Å along the Cu–N vector) this charge remains, at least partially, in the Wigner–Seitz cell and is part of the integration. The Cu adatom is at no point uncoordinated and negatively charged. However, in establishing the coordination bonds it obtains an approximate −1 charge from the substrate so that it can serve as a donor to each of its ligands (of approximate +1/3 charge) without becoming positively charged itself. Solely in this characteristic does it resemble an anion. As negatively charged copper centers do not generally occur in the solution phase, for comparison we computed the lowest energy conformation of free $[Cu^x(\text{dicyanobenzene})_3]$ complexes with $x=-1$, 0, $+1$ using (HF/3-21G*) in Spartan 06.[14] While a trigonal-planar configuration is stable for all copper oxidation states, a coplanar arrangement of the ligand aromatic moieties is stable exclusively for $x=-1$, for which the Cu–N bonds are shortest and, not surprisingly, strongest, in further support of the favored character of the configuration detected for Cu(111).

Figure 4 shows on the left two perpendicular views (parallel and perpendicular to the Cu(111) plane) of the charge density surrounding an adatom in the β phase. Figure 4, right, shows the excess (red) and missing (blue) charge density compared to the same fixed surface setup, after artificial removal of the Cu adatom. The high charge density at the location of the adatom is apparent, and also the donating character of the substrate (bottom). Note the

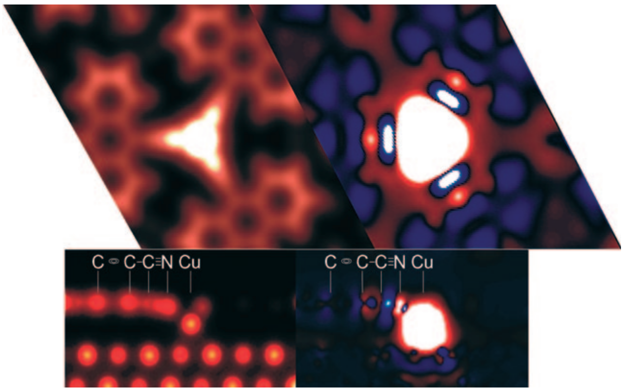

Figure 4. Left: charge density around a copper adatom coordinated by three DCA molecules seen from parallel (top) and perpendicular (bottom) to the Cu(111) plane. Right: changes in charge density after artificial removal of the Cu adatom (excess charge shown in red, deficit in blue). Charge transfer from the substrate and partial conversion of the cyano triple bond into a double bond, and of the C–C single bond to a double bond is apparent.

decrease in charge density immediately next to the nitrogen atom, as a result of the coordination of its lone pair to copper, the reduced charge density at the $N\equiv C$ bond and the emerging π bond of the nitrile group to the ring system, converting the original $N\equiv C$-anthracene bonding arrangement partially towards a Cu−N=C=anthracene sequence, in further support of the profound dative impact of N–Cu coordination on the charge density in the molecule. The calculated electronic density of states around the copper and the nitrogen atom as a function of energy, decomposed in s, p, and d character, are shown in the Supporting Information.

In conclusion, we present a coordination network, formed at a metal surface in a system facile to prepare because the required metal centers can be released in a measured fashion from the substrate by simple annealing. Analysis of the charge density in this system suggests that metal adatoms can have a pronounced donating character despite the electron deficiency of uncoordinated adatoms. The notion that metal adatoms present an anionic character in their interaction with molecular adsorbates could have significant and widespread implications (for example, in heterogeneous catalysis). For instance, the concept that negative charging is at the origin of the high activity of gold nanoparticles in CO oxidation is already a topic of discussion.[15] Further examples of this behavior need to be found before any generalizations can be made.

Experimental Section

We use a home-built variable-temperature scanning tunneling microscope (STM) operated in ultra-high vacuum. Cu(111) sample preparation involved sputtering (Ar^+, 3 kV) and annealing of a single crystal followed by cooling to liquid nitrogen temperatures within the STM. Deposition onto the cold sample occurred from a glass capillary attached to the vacuum chamber through a gate valve in a line-of-sight fashion while controlling the deposition rate through measurement of the pressure in the vacuum chamber.

Density functional theory calculations of the electronic and geometric structures and adsorption energies of DCA on Cu(111) were carried out using the Vienna Ab Initio Simulation Package (VASP)[16] implementing the generalized gradient approximation (GGA) for the exchange-correlation functional[17] and the plane-wave pseudopotential method.[18] Projector-augmented wave (PAW)[19] pseudopotentials were used for all atoms in the system. The cutoff energy for the plane-wave expansion is taken to be 400 eV and, depending on the unit cell size, a $2\times 2\times 1$ Monkhorst-Pack *k*-point mesh or a single point are used in Brillouin zone sampling[20] to obtain converged results for the total energy of the system. We typically restricted our calculation super cell to two or three substrate (copper) layers so as to keep the total number of substrate atoms in the supercell to approximately 100 for computational feasibility. During lattice relaxation, all adsorbate and top-layer substrate atoms were allowed to move in all directions. The structures and energies that are shown in this study result from relaxation of the forces acting on each atom to better than $0.01\ \mathrm{eV}\,\text{Å}^{-1}$. The physisorbed adsorption energy of DCA is approx. 0.4 eV. We wish to caution, however, that GGA occasionally underestimates the absolute binding energy in physisorbed systems.[21]

Received: May 31, 2008
Published online: August 29, 2008

Keywords: coordination modes · density functional calculations · scanning probe microscopy · structure elucidation · surface chemistry

[1] a) U. Schlickum, R. Decker, F. Klappenberger, G. Zoppellaro, S. Klyatskaya, M. Ruben, I. Silanes, A. Arnau, K. Kern, H. Brune, J. V. Barth, *Nano Lett.* **2007**, *7*, 3813–3817; b) O. M. Yaghi, M. O'Keeffe, N. W. Ockwig, H. K. Chae, M. Eddaoudi, J. Kim, *Nature* **2003**, *423*, 705–714; c) M. Ruben, J. Rojo, F. J. Romero-Salguero, L. H. Uppadine, J. M. Lehn, *Angew. Chem.* **2004**, *116*, 3728–3747; *Angew. Chem. Int. Ed.* **2004**, *43*, 3644–3662; d) A. Dmitriev, H. Spillmann, N. Lin, J. V. Barth, K. Kern, *Angew. Chem.* **2003**, *115*, 2774–2777; *Angew. Chem. Int. Ed.* **2003**, *42*, 2670–2673; e) J. V. Barth, G. Costantini, K. Kern, *Nature* **2005**, *437*, 671–679; f) N. Zhu, T. Osada, T. Komeda, *Surf. Sci.* **2007**, *601*, 1789–1794; g) S. L. Tait, Y. Wang, G. Costantini, N. Lin, A. Baraldi, F. Esch, L. Petaccia, S. Lizzit, K. Kern, *J. Am. Chem. Soc.* **2008**, *130*, 2108–2113; h) T. Classen, M. Lingenfelder, Y. Wang, R. Chopra, C. Virojanadara, U. Starke, G. Costantini, G. Fratesi, S. Fabris, S. de Gironcoli, S. Baroni, S. Haq, R. Raval, K. Kern, *J. Phys. Chem. A* **2007**, *111*, 12589–12603; i) A. Breitruck, H. E. Hoster, C. Meier, U. Ziener, R. J. Behm, *Surf. Sci.* **2007**, *601*, 4200–4205; j) H. M. Zhang, Z. X. Xie, L. S. Long, H. P. Zhong, W. Zhao, B. W. Mao, X. Xu, L. S. Zheng, *J. Phys. Chem. C* **2008**, *112*, 4209–4218; k) S. Stepanow, N. Lin, D. Payer, U. Schlickum, F. Klappenberger, G. Zoppellaro, M. Ruben, H. Brune, J. V. Barth, K. Kern, *Angew. Chem.* **2007**, *119*, 724–727; *Angew. Chem. Int. Ed.* **2007**, *46*, 710–713.

[2] A. P. Seitsonen, M. Lingenfelder, H. Spillmann, A. Dmitriev, S. Stepanow, N. Lin, K. Kern, J. V. Barth, *J. Am. Chem. Soc.* **2006**, *128*, 5634–5635.

[3] K. L. Wong, G. Pawin, K. Y. Kwon, X. Lin, T. Jiao, R. Fawcett, U. Solanki, L. Bartels, S. Stolbov, T. S. Rahman, *Science* **2007**, *315*, 1391–1393.

[4] K. Y. Kwon, K. L. Wong, G. Pawin, L. Bartels, S. Stolbov, T. S. Rahman, *Phys. Rev. Lett.* **2005**, *95*, 166101.

[5] G. Pawin, U. Solanki, K. Y. Kwon, K. L. Wong, X. Lin, T. Jiao, L. Bartels, *J. Am. Chem. Soc.* **2007**, *129*, 12056–12057.

[6] G. Pawin, K. L. Wong, K. Y. Kwon, L. Bartels, *Science* **2006**, *313*, 961–962.

[7] The Supporting Information section contains a figure.

[8] J. Kroger, H. Jensen, R. Berndt, R. Rurali, N. Lorente, *Chem. Phys. Lett.* **2007**, *438*, 249–253.

[9] D. Venkataraman, Y. H. Du, S. R. Wilson, K. A. Hirsch, P. Zhang, J. S. Moore, *J. Chem. Educ.* **1997**, *74*, 915–918.

[10] T. Pretsch, I. Brudgam, H. Hartl, *Z. Anorg. Allg. Chem.* **2003**, *629*, 942–944.

[11] C. Ghosh, A. Kara, T. Rahman, *Surf. Sci.* **2002**, *502*, 519–526.

[12] The Wigner–Seitz cell around an atom in a lattice is the locus of points closer to it than to any other lattice atom, thus describing the volume associated with one atom in a lattice.

[13] Found by calculating the charge density for the same fixed surface and adsorbate setup without the copper adatom present.

[14] Wavefunction Inc., Irvine, CA.

[15] a) S. Chretien, H. Metiu, *J. Chem. Phys.* **2007**, *126*, 104701; b) A. S. Worz, U. Heiz, F. Cinquini, G. Pacchioni, *J. Phys. Chem. B* **2005**, *109*, 18418–18426.

[16] G. Kresse, J. Hafner, *Phys. Rev. B* **1993**, *47*, 558–561.

[17] J. P. Perdew, Y. Wang, *Phys. Rev. B* **1992**, *45*, 13244–13249.

[18] M. C. Payne, M. P. Teter, D. C. Allan, T. A. Arias, J. D. Joannopoulos, *Rev. Mod. Phys.* **1992**, *64*, 1045–1097.

[19] D. Vanderbilt, *Phys. Rev. B* **1990**, *41*, 7892–7895.

[20] H. J. Monkhorst, J. D. Pack, *Phys. Rev. B* **1976**, *13*, 5188–5192.

[21] X. Wu, M. C. Vargas, S. Nayak, V. Lotrich, G. Scoles, *J. Chem. Phys.* **2001**, *115*, 8748–8757.